Available online at www.sciencedirect.com

SCIENCE DIRECT

Biochimica et Biophysica Acta 1721 (2005) 1–8

BIOCHIMICA ET BIOPHYSICA ACTA
BBA

http://www.elsevier.com/locate/bba

Structural characterization of human liver heparan sulfate

Preeyanat Vongchan[a], Mohamad Warda[b], Hidenao Toyoda[c], Toshihiko Toida[c], Rory M. Marks[d], Robert J. Linhardt[b,e,*]

[a]*Faculty of Medicine, Chiang Mai University, Thailand*
[b]*Department of Biochemistry, Faculty of Veterinary Medicine, Cairo University, Cairo, Egypt*
[c]*Graduate School of Pharmaceutical Science, Chiba University, Chiba, Japan*
[d]*Department of Internal Medicine, University of Michigan, Ann Arbor, MI 48109, USA*
[e]*Department of Chemistry, Biology and Chemical Engineering, Rensselaer Polytechnic Institute, Troy, NY 12180, USA*

Received 7 August 2004; received in revised form 24 September 2004; accepted 28 September 2004
Available online 20 October 2004

Abstract

The isolation, purification and structural characterization of human liver heparan sulfate are described. ^{1}H-NMR spectroscopy demonstrates the purity of this glycosaminoglycan (GAG) and two-dimensional ^{1}H-NMR confirmed that it was heparan sulfate. Enzymatic depolymerization of the isolated heparan sulfate, followed by gradient polyacrylamide gel, confirmed its heparin lyase sensitivity. The concentration of resulting unsaturated disaccharides was determined using reverse phase ion-pairing (RPIP) HPLC with post column derivatization and fluorescence detection. The results of this analysis clearly demonstrate that the isolated GAG was heparan sulfate, not heparin. Human liver heparan sulfate was similar to heparin in that it has a reduced content of unsulfated disaccharide and an elevated average sulfation level. The antithrombin-mediated anti-factor Xa activity of human liver heparan sulfate, however, was much lower than porcine intestinal (pharmaceutical) heparin but was comparable to standard porcine intestinal heparan sulfate. Moreover, human liver heparan sulfate shows higher degree of sulfation than heparan sulfate isolated from porcine liver or from the human hepatoma Hep 2G cell line.

Keywords: heparan sulfate; Human liver; Structure; Glycosaminoglycan; Proteoglycan

1. Introduction

Heparan sulfate is the glycosaminoglycan (GAG) component of heparan sulfate proteoglycans (PGs) found both in the extracellular matrix and on the cell surface of animal cells [1,2]. Heparan sulfate-PG consists of a core protein, commonly associated with either the glypican or syndecan families, to which one or more heparan sulfate-GAG chains are attached [3,4]. Heparan sulfate-PGs may represent one of the most biologically important glyco-conjugates, playing essential roles in a variety of different events at the molecular level [5–8]. Heparan sulfate-PG in liver acts as a critical receptor for apoE and is involved in lipid metabolism [9,10] and is possibly involved in some of the pathology associated with Alzheimer's disease [11,12]. Human liver is also a target for a number of pathogens and heparan sulfate has been demonstrated in several cases to play a pivotal role in infectivity [13–15].

The liver is known to be a rich source of GAGs. Indeed, heparin was named based on its initial isolation from canine liver [16]. Rat liver heparan sulfate-PG [17] and bovine and porcine liver heparan sulfate-GAG [18,19] have been isolated, characterized and shown to be highly sulfated. While heparin is often referred to as a highly sulfated subtype of heparan sulfate, it is distinctive in that it is an intracellular GAG found in granulated cells (i.e., mast cells) and is biosynthesized on the serglycin core protein [20,21]. In contrast, heparan sulfate is an extracellular GAG,

* Corresponding author. Department of Chemistry, Biology and Chemical Engineering, Rensselaer Polytechnic Institute, Troy, NY 12180, USA. Tel.: +1 518 276 3404; fax: +1 518 276 3405.
E-mail address: linhar@rpi.edu (R.J. Linhardt).

0304-4165/$ - see front matter © 2004 Elsevier B.V. All rights reserved.
doi:10.1016/j.bbagen.2004.09.007

suggesting its importance as a receptor or coreceptor for various heparin-binding proteins [2].

Specific highly sulfated heparan sulfate sequences in the liver, implicated in binding apoE [9], also appear to bind tightly to surface proteins of the malaria circumsporozoite [22], dengue virus [23] and hepatitis C virus [15], all pathogens showing tropism for the liver. While the structure of heparan sulfate from the human hepatoma (Hep2G) cell line [24] has been studied [15], to our knowledge heparan sulfate from human liver has not been previously isolated and characterized. Structural characterization of the human liver heparan sulfate should help to solve some questions concerning the interaction, at the molecular level, of heparan sulfate in the normal hepatic cells with its protein-based receptors and ligands and with pathogen proteins.

The current study focuses on the structural characterization of heparan sulfate isolated from human liver. Partial characterization of the heparan sulfate-PG in human liver as well as the extensive characterization of heparan sulfate-GAG is reported. This improved structural knowledge of the heparan sulfate in normal hepatic cells is a beginning in our glycomic effort to establish an understanding at the molecular level of heparan sulfate–protein interactions [25] required in cell signaling, lipoprotein trafficking and infectious disease.

2. Materials and methods

Human livers were supplied by organ donation organization (National Disease Research Interchange; National Resource Center). Three human liver samples, without underlying liver disease, obtained from different donors were used in the study. Each sample (~350 g fresh weight) was divided into two equal portions for isolation of heparan sulfate-PG and heparan sulfate-GAG.

2.1. Preparation of heparan sulfate-PG from human liver

The purification of human liver heparan sulfate-PG was based on the previously reported purification of murine liver heparan sulfate-PG [17] and bovine brain heparan sulfate-PG [26]. Briefly, frozen liver samples from three human donors were cut into small pieces and homogenized overnight in aqueous 4 M guanidinium chloride containing 2% (v/v) Triton X-100, 50 mM sodium acetate, 0.1 M 6-amino-hexanoic acid, 20 mM benzamidine hydrochloride, 10 mM EDTA, 5 mM *N*-ethylmaleimide and 0.5 mM PMSF, pH 5.0. The insoluble residue is removed by filtration and protein is precipitated from soluble extract with final 10% of trichloroacetic acid for 30 min at 4 °C. The supernatant is then neutralized to pH 7.0 with Na_2CO_3 and concentrated to less than one third of its volume by reverse osmosis using polyethylene glycol 8000 following with dialysis against 20 mM Tris/HCl pH 8.0 containing 8 M urea, 0.15 M NaCl and 0.5% (v/v) Triton X-100, using membranes having a molecular mass cutoff (MMCO) of 3500 Da. The anion components are adsorbed onto 500-ml DEAE-Sephacel beads at 4 °C overnight and loaded into 2.5×75-cm column. The column is washed with 20 mM piperazine/HCl pH 5.0 containing 6 M urea, 0.15 M NaCl and 5.5% (v/v) Triton X-100 and eluted using a salt gradient at 40 ml/hr. All fractions are precipitated in final 85% of absolute methanol and resuspened in 500 μl of 50 mM Tris/HCl pH 8.0 containing 50 mM NaCl, 0.1% Triton X-100 and protease inhibitors and assayed by the carbazole reaction. Pooled fractions are then dialyzed against the same buffer and concentrated 30-fold using pressure filtration through an Amicon Ultrafree Biomax-5 filter before precipitating at −20 °C for 12 h with 3 volumes of 1.3% (w/v) of potassium acetate in 95% ethanol in the presence of chondroitin sulfate carrier. The precipitate is recovered and redissolved in 30 mM Tris/HCl pH 7.5 containing 4 M guanidinium chloride, 0.5% CHAPS, and separated on a Sepharose CL-6B column (1.0×107 cm), monitored by 1,9-dimethylmethylene blue, and analyzed on 8% (w/v acrylamide) SDS/PAGE visualized by Alcian blue staining followed by silver staining.

2.2. Preparation of heparan sulfate-GAG from human liver

Liver samples from three human donors were cut into small pieces (<1 mm) and crushed with dry ice into very fine homogenized powder using a mortar and pestle. Fat was removed by washing the powdered tissues with chloroform/methanol mixtures (2:1, 1:1, 1:2 (v/v)). The defatted materials were dried under vacuum and stored at −40 °C until further use. The dried, defatted tissues were each suspended in 0.05 M Tris acetate buffer (pH 8.0) and digested for 48 h by actinase E 10 mg/g (Kaken Pharm., Tokyo, Japan) at 50 °C. The proteolyzed homogenates were placed in a boiling water bath for 15 min to deactivate the protease and then centrifugated (2500×*g*) for 30 min at 4 °C. The recovered supernatant was treated using sodium borohydride (1% w/v) under mild alkaline conditions (0.2 M NaOH at 4°C overnight) to remove the GAG chain from its core protein by β-elimination. After neutralization (with 0.2 M HCl), perchloric acid (75%) was added to obtain a final concentration of 5% (v/v). Precipitated protein was removed by centrifugation (10,000×*g*) for 30 min at 4 °C and the supernatant was recovered, dialyzed in cellulose membrane tubing (molecular weight cutoff (MWCO), 3500) against distilled water for 2 successive days at 4 °C. The retentate was recovered and cetylpyridinium chloride (CPC) was added (0.1% w/v) and the mixture was allowed to stand for 3 h at 4 °C, centrifugation was performed (2500×*g*) at 4 °C for 15 min and the precipitate was recovered and washed two times with 0.1% CPC solution and recovered each time by centrifugation. Finally, the recovered precipitate was dissolved in 2.5 M NaCl and the crude GAG was recovered by methanol (85% v/v) precipitation. After standing overnight at 4 °C, the crude GAG precipitate was

recovered by centrifugation (2500×*g*) at 4 °C for 15 min, dialyzed (3500 MWCO) and freeze-dried.

Crude human liver GAGs were treated with chondroitin lyase ABC (Sigma, MO, USA, 2 m-unit/mg in 50 mM sodium acetate, pH 8) at 37 °C for 24 h in sealed tubes to remove all traces of galactosaminoglycans. The action of the enzyme was confirmed using chondroitin sulfate A (Sigma). After chondroitinase digestion, the reactions were terminated by heating in a boiling water bath 5 min and the digested samples were desalted using a Sephadex G-10 microanalysis desalting spin column (Harvard Apparatus Inc. MA, USA) and freeze-dried. Next the freeze-dried sample (0.3–5 mg) was dissolved in 20 mM Tris/HCl buffer (pH 8) containing 2 mM magnesium chloride and digested with endonuclease (2.5 units/mg, Sigma) for 12 h at 37 °C [27] to remove any nucleic acid contaminants. After endonuclease digestion, the reaction was terminated by heating in boiling water bath for 5 min and the samples were desalted using a Sephadex G-10 microanalysis desalting spin columns and the resulting purified human liver heparan sulfate was freeze-dried.

2.3. PAGE and gradient polyacrylamide gel electrophoresis

Heparan sulfate-PG and core protein preparations were subjected to discontinuous SDS-PAGE (8×10-cm pre-cast gels, 10% acrylamide (w/v), at 200 V for 45 min, Bio-Rad unit equipped with model 1420B power source, Richmond, CA) under reducing conditions. Protein bands were visualized with zinc staining (GelCode E-Zinc Reversible Stain, Pierce Biotechnology, Rockford, IL, USA) and the purity was determined from silver staining. Core protein was visualized with zinc stain staining or transferred to PVDF membrane (0.22 μm, Bio-Rad) using a Hoefer TE 70 Semi-Phor Semi-Dry transfer unit (Amersham Biosciences, Piscataway, NJ, USA). Blots were probed with anti-glypican and visualized using ECL Plus Western Blotting Reagents (Amersham Biosciences), probed with stub antibodies against heparan sulfate-PGs [26]. The molecular weight of heparan sulfate-PG core protein was determined using protein standards. heparan sulfate-GAG was analyzed by polyacrylamide linear gradient resolving gels (14×28 cm, 12–22% acrylamide) prepared and run as described previously [19]. The average molecular mass of heparan sulfate-GAG chains was determined by comparing with a banding ladder of heparin oligosaccharide standards prepared from bovine lung heparin and tetrasaccharide marker was added to identify the bands (using UN-Scan-IT gel, automated digitizing system, version 4.3 for Macintosh, Silk Scientific, CA, USA).

2.4. Chemical characterization of heparan sulfate-GAG using ^{1}H-NMR analysis

NMR spectroscopy was performed on the purified heparan sulfate samples dissolved in $^{2}H_2O$ (99.96 at.%), filtered through a 0.45-μm syringe filter (Millipore, Bedford, MA, USA), freeze-dried twice with $^{2}H_2O$ to remove exchangeable protons and transferred to Shigemi tubes. One-dimensional (1D) ^{1}H-NMR experiments were performed on a Jeol GSX A500.

2.5. Enzymatic depolymerization of heparan sulfate-GAGs

The purified heparan sulfate samples were next treated with an equi-unit mixture of heparinase lyase I, II, III to perform disaccharide analysis [28]. Dried samples were dissolved in buffer (50 mM sodium phosphate buffer, pH 7.1 and 100 mM NaCl) at a concentration of 1 mg/100 ml. Each heparin lyase was added at three time periods, 0, 8 and 16 h, to a final concentration of 0.02 m-IU/mg GAG dry weight. The reaction mixture was incubated on membrane of Ultrafree ®-MC centrifugal filter spin membrane (5000 nominal molecular weight limit (NMWL), Amicon Millipore) at 37 °C over a period of over 24 h. The disaccharides were recovered from the spin column by centrifugation (12,000 rpm) for 30 min at 4 °C.

2.6. Analysis of heparan sulfate-GAG

The following standard unsaturated disaccharides from heparan sulfate were purchased from Sigma: ΔUA-GlcNAc, ΔUA-GlcNS, ΔUA-GlcNAc6S, ΔUA2S-GlcNAc, ΔUA-GlcNS6S, ΔUA2S-GlcNS, ΔUA2S-GlcNAc6S, ΔUA2S-GlcNS6S (for detailed structure see, Ref. [19]), and heparan sulfate (from bovine kidney). Heparin lyase I (EC 4.2.2.7, heparinase I, heparinase), heparin lyase II (heparinase II, heparitinase II), and heparin lyase III (EC 4.2.2.8, heparinase III, heparitinase I) were obtained from Sigma and Seikagaku America. Senshu Pak Docosil (4.6×150 mm; particle size, 5 μm) was obtained from Senshu Scientific (Tokyo, Japan). Ultrafree-MC DEAE and Biomax-5 (5000 normal molecular weight limit) were obtained from Millipore. All other chemicals used were of analytical reagent grade.

The chromatographic equipment included a gradient pump (L-7000), a chromato-integrator (D-7500) from Hitachi Seisakusho (Tokyo), a double plunger pump for the reagent solution (Shimamura Seisakusho, Tokyo), a sample injector with a 20-μl loop (model 7125, Reodyne, Rohnert Park, CA), a fluorescence spectrophotometer (Jasko FL980S) from Nipponn Bunko (Tokyo), and a dry reaction bath (FH-40) from Shimamura Seisakusho.

Unsaturated disaccharides produced enzymatically from heparan sulfate were determined by a reversed-phase ion-pair chromatography with sensitive and specific post-column detection [29]. A gradient was applied at a flow rate of 1.1 ml/min on a Senshu Pak Docosil (4.6×150 mm) at 55 °C. The eluents used were as follows: A, H_2O; B, 0.2 M sodium chloride; C, 10 mM tetra-*n*-butylammonium hydrogen sulfate; D, 50% acetonitrile. The gradient program was as follows: 0–10 min, 1–4% eluent B; 10–11 min, 4–15% eluent B; 11–20 min, 15–25% eluent B; 20–22 min, 25–53% eluent B; 22–29 min, 53% eluent B; equilibration with 1% B for 20

min. The proportions of eluent C and D were constant at 12% and 17%, respectively. To the effluent were added aqueous 0.5% (w/v) 2-cyanoacetamide solution and 0.25 M sodium hydroxide at the same flow rate of 0.35 ml/min by using a double plunger pump. The mixture passed through a reaction coil (internal diameter, 0.5 mm; length, 10 m) set in a dry reaction temperature-controlled bath at 125 °C and a following cooling coil (internal diameter, 0.25 mm; length, 3 m). The effluent was monitored fluorometrically (excitation, 346 nm; emission, 410 nm).

2.7. Anticoagulant activity assay

The anticoagulant activity of heparan sulfate-GAG was analyzed by determining its ability to catalyze antithrombin-mediated inactivation of factor Xa. A heparin assay kit (Sigma Diagnostics) was used to determine anti-factor Xa activity. Both factor Xa and antithrombin were present in excess and, thus, the inhibition of factor Xa was directly proportional to the limiting concentration of heparan sulfate-GAG. Residual factor Xa activity, measured with factor Xa-specific chromogenic substrate, was inversely proportional to the anticoagulant activity.

3. Results

The heparan sulfate-PG obtained from human liver tissue had a molecular weight of >200,000 as estimated by SDS-PAGE (not shown). Treatment with an equi-unit mixture of heparin lyases gave a prominent band of ~61 kDa by zinc staining (Fig. 1, Panel A). Electroelution of this band (prior to staining) onto PVDF membrane and visualization by Western blot analysis with anti rat glypican antibody (Fig. 1B) [30] or heparan sulfate-PG stub antibody (not shown) gave a band at 61 kDa. Sequence analysis of this heparan sulfate-PG failed possibly due to a blocked N-terminus or multiple N-termini. Our focus next turned to the preparation of heparan sulfate-GAG from human liver tissue for structural characterization. Human liver heparan sulfate-GAG was obtained in a yield of ~0.08 mg/gm wet tissue weight. Gradient PAGE analysis of human liver heparan sulfate-GAG (Fig. 2A, lane 7) gave a broad band on Alcian blue staining similar to that observed for porcine intestinal heparan sulfate (lane 1) and porcine intestinal heparin (lane 5). Treatment with heparin lyases resulted in the disappearance of the broad bands corresponding to heparan sulfate and heparin (Fig. 2A, lanes 2, 6 and 8). In the case of heparin, heparin lyase treatment results in small highly sulfated oligosaccharide products that still contain sufficient negative charge (≥2 sulfo groups [31] to stain with Alcian blue (Fig. 2A, lane 6). In contrast, both human liver and porcine intestinal heparan sulfate are insufficiently sulfated to afford products that stain with Alcian blue. Gradient PAGE analysis of intact heparin and heparan sulfate was also used to estimate average molecular weight (MW) [32]. A banding ladder prepared from the partial heparinase catalyzed depolymerization of bovine lung heparin was used as molecular weight markers. A reading frame was established in this oligosaccharide mixture by using a pure, heparin-derived, tetrasaccharide standard, corresponding to ΔUA2S (1→4)-β-D-GlcNS6S (1→4)-α-L-IdoA2S (1→4)-β-D-GlcNS6S [32,33] (Fig. 2A, lanes 3 and 4). A plot of log MW as a function of migration distance (Fig. 2B) was used to determine the average molecular weight of the broad bands in Fig. 2A, lanes 1, 2, 5, 6, 7 and 8 [32]. Porcine intestinal heparin and porcine intestinal heparan sulfate both showed an average molecular weight of <20,000, consistent with those previously reported for heparin and heparan sulfates [28,32]. In contrast, human liver heparan sulfate had a molecular weight of ~24,000. Analysis of the charge density of human liver heparan sulfate by SAX chromatography showed that it contained two populations of chains. The major population (85%) had a low level of sulfation consistent with heparan sulfate obtained from non-liver sources, while the minor population (15%) was highly sulfated. The behavior of this minor population of GAG chains on SAX chromatography and its level of sulfation (~1.3 sulfo groups/disaccharide compared to 0.8 for the major population of chains and 2.2 to 2.7 for heparin) suggest that it is a highly sulfated heparan sulfate and not a heparin. Because of the limited amounts of sample, the total heparan sulfate, containing both undersulfated and highly sulfated chains, was analyzed.

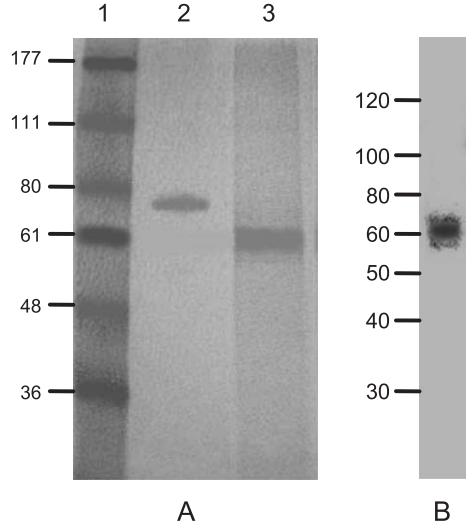

Fig. 1. PAGE analysis of heparan sulfate-PG following heparin lyase treatment. Panel A. Zinc stained gel for protein visualization. Lane 1, the arrows indicate the molecular weight of each molecular weight marker band; lane 2, bovine serum albumin standard (68 kDa); and lane 3, heparan sulfate-PG after treatment with heparin lyases giving a band at 61 kDa. Panel B. Immunoblot using rabbit anti-rat glypican of heparan sulfate-PG after treatment with heparin lyases.

Following exchange with $^{2}H_2O$, human liver heparan sulfate-GAG was examined by high-filed NMR spectroscopy. Assignments of signals were made using 1D ^{1}H-NMR (Fig. 3). In comparison to previously published

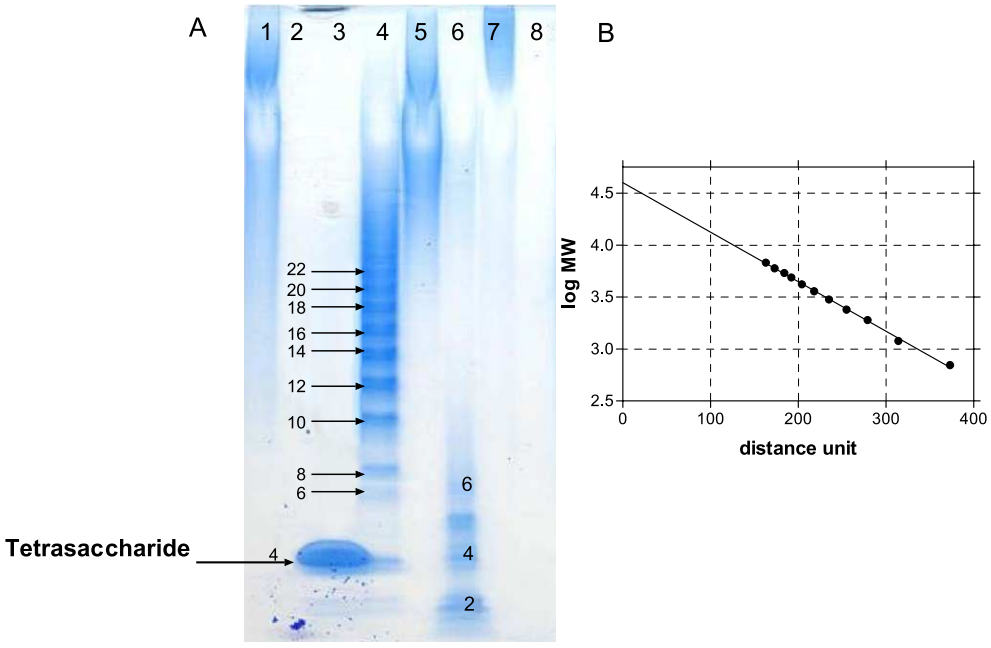

Fig. 2. Panel A. Gradient PAGE analysis with Alcian blue staining of GAG samples before and after treatment with heparin lyases. Lane 1 is intact porcine intestinal heparan sulfate; lane 2 is porcine intestinal heparan sulfate after treatment with heparin lyase 1, 2 and 3; lane 3 is heparin hexasulfated tetrasaccharide standard indicated by the arrow [33]; lane 4 is heparin-derived oligosaccharide standards enzymatically prepared from bovine lung heparin—the numbers indicate their degree of polymerization [32]; lane 5 is intact porcine heparin; lane 6 is porcine intestinal heparin after heparin lyase treatment; lane 7 is human liver heparan sulfate; lane 8 is human liver heparan sulfate after heparin lyase treatment. Panel B. A plot of log MW of bovine lung heparin-derived oligosaccharide standards as a function of migration distance of each oligosaccharide from which the average molecular weight of each GAG can be calculated.

spectra of porcine intestinal heparin [28] and porcine liver heparan sulfate [19], human liver heparan sulfate showed a typical resonance for heparan sulfate from animal organs, for example, there are several small signals around 4.5–5.4 ppm, which is also shown in porcine liver heparan sulfate (Fig. 3). These signals might have resulted from complex sulfation patterns of heparan sulfate. In contrast, the GlcA H-2 signal at 3.3 ppm of human liver heparan sulfate is larger than that found in porcine intestine heparan sulfate (Fig. 3). This observation suggests that the content of GlcA residues in human liver heparan sulfate is conspicuously higher.

Disaccharide compositional analysis of human liver heparan sulfate following digestion with an equi-unit mixture heparin lyases 1, 2 and 3 was determined by reversed phase high performance liquid chromatography

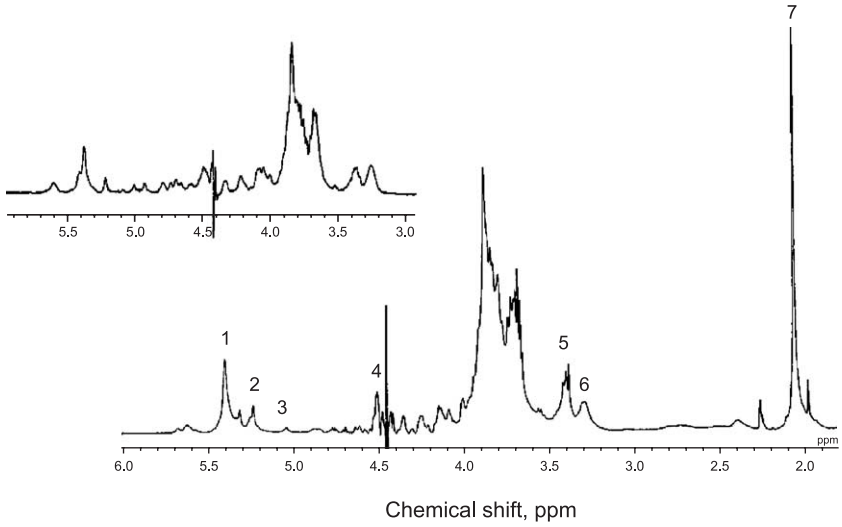

Fig. 3. 1D ^{1}H-NMR spectroscopy of human liver heparan sulfate. Inset: heparan sulfate from porcine intestinal mucosa. Signals: 1, GlcNX H-1; 2, Ido2S H-1; 3, IdoA H-1; 4, GlcA H-1 (overlapped with HOD signal irradiated); 5, GlcA H-2; 6, GlcNS H-2; 7, N-acetyl methyl signal of GlcNAc. A sharp singlet signal of N-acetyl methyl may indicate that the sequence of GlcNAc residues in human liver heparan sulfate is regulated at the positions next to GlcA residues.

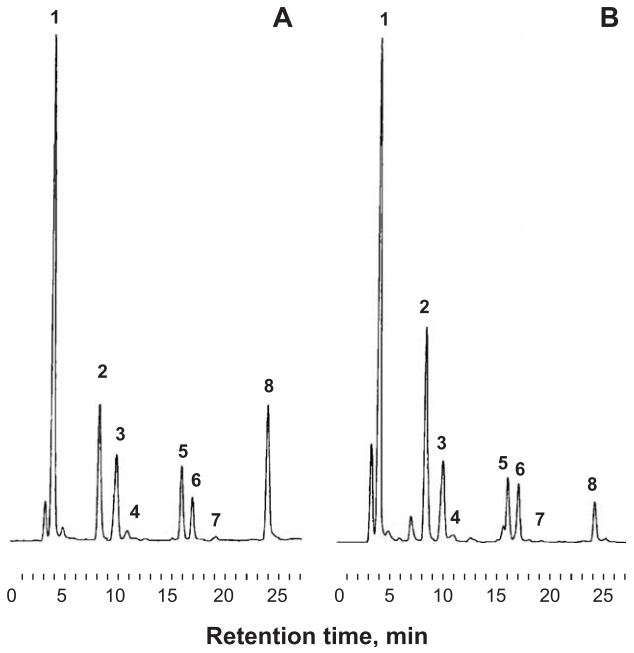

Fig. 4. Disaccharide analysis of heparin lyase 1, 2 and 3 treated (A) human liver heparan sulfate and (B) porcine intestine heparan sulfate by RPIP HPLC using post column derivatization and fluorescence detection. The numbers of peaks represent the different disaccharides (see Table 1).

(RPIP-HPLC) with post column derivation and fluorescence detection (Fig. 4). A mixture of eight heparin oligosaccharides of the structure: 1. ΔUA(1→4)GlcNAc; 2. ΔUA(1→4)GlcNS; 3. ΔUA(1→4)GlcNAc6S; 4. ΔUA2S(1→4)GlcNAc; 5. ΔUA(1→4)GlcNS6S; 6. ΔUA2S(1→4)GlcNS; 7. ΔUA2S(1→4)GlcNAc6S; 8. ΔUA2S(1→4)GlcNS6S (where ΔUA is 4-deoxy-α-L-*threo*-hex-4-enopyranosyl uronic acid, GlcN is 2-amino-2-deoxyglucopyranose, Ac is acetyl and S is sulfo) is shown in Fig. 4. The same analysis performed on porcine intestine heparan sulfate is also presented for comparison purposes. The identity of each disaccharide in was confirmed by co-injection with individual disaccharide standards. Table 1 compares the disaccharide composition of human liver heparan sulfate-GAG to porcine intestinal heparin, porcine intestinal heparan sulfate [28], bovine kidney heparan sulfate porcine liver heparan sulfate [19] and Hep2G-derived heparan sulfate [15].

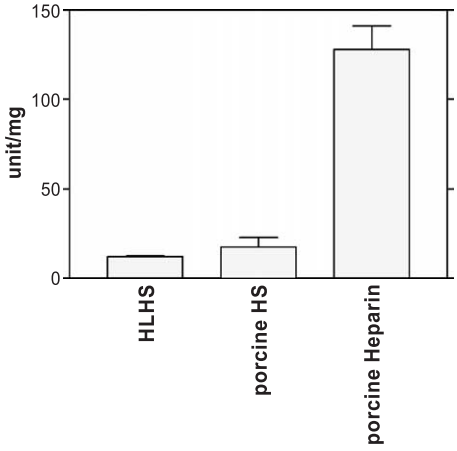

Fig. 5. Comparison of anti-factor Xa activities of human liver heparin sulfate, porcine intestinal heparan sulfate and porcine intestinal heparin. The anti-factor Xa activity of heparin is significantly higher ($P<0.01$) than that of human liver heparan sulfate and porcine intestinal heparan sulfate. There is no significant difference between human liver heparan sulfate and porcine intestinal heparan sulfate anti-factor Xa activity. The error bar is mean±S.E. of at least five determinations.

The anticoagulant activity of human liver heparan sulfate (Fig. 5), determined by anti-factor Xa assay, showed that human liver heparan sulfate had significantly lower anti-factor Xa activity than porcine intestinal heparin and comparable activity to porcine intestinal heparan sulfate.

4. Discussion

Heparan sulfate is a GAG having a structure similar to heparin but generally with a reduced content of *O*-sulfo and *N*-sulfo groups, a larger ratio of GlcA to IdoA and a greater amount of sequence heterogeneity [19,34]. Heparan sulfate is often found covalently linked to the membrane proteins syndecan and glypican where it provides binding sites for numerous protein ligands and receptors, regulating diverse biological processes [25,35], including growth control, signal transduction cell adhesion, hemostasis [43] and lipid metabolism. Extracellular heparan sulfate has been impli-

Table 1
Disaccharide analysis of heparin and various heparan sulfate

Source	(1) ΔUA-GlcNAc[a]	(2) ΔUA-GlcNS	(3) ΔUA-GlcNAc6S	(4) ΔUA2S-GlcNAc	(5) ΔUA-GlcNS6S	(6) ΔUA2S-GlcNS	(7) ΔUA2S-GlcNAc6S	(8) ΔUA2S-GlcNS6S[a]
Porcine intestinal heparin	3.1	3.6	14.5	1.2	24.9	12.4	nd	40.3
Human liver heparan sulfate	37.3	15.5	9.8	1.2	7.8	5.9	0.7	21.8
Porcine liver heparan sulfate [19]	47.9	10.8	10.2	nd	5.6	4.4	nd	21.2
Porcine intestinal heparan sulfate	40.6	25.8	10.8	0.7	6.5	8.4	0.2	7.0
Hep2G cell heparan sulfate [15]	46.1	22.9	9.9	2.9	6.2	4.4	0.6	6.7
Bovine kidney heparan sulfate [19]	56.4	15.9	12.8	nd	4.2	7.2	2.2	1.3

[a] The values are expressed in mol%. The range observed for heparan sulfate obtained across a wide range of tissues for these two critical disaccharides can be found in Ref. [19]. Unsulfated disaccharide (1) ranges from 45% to 78% and trisulfated disaccharide (8) from <1% to 21% with sulfation level ranging from 0.26 to 1.05 sulfo groups/disaccharide.

cated in a number of pathological processes through its binding to the surface proteins of various pathogens including malaria circumsporozoite [22], human immune deficiency virus [35], herpes simplex virus [36], dengue virus [23] and hepatitis C virus [15]. Of particular interest to our laboratory are malaria, dengue virus and hepatitis C virus, as they are all pathogens that target the liver.

Human liver proteoglycan isolated and partially characterized in this work had an apparent molecular weight of >200 kDa with a 60-kDa core protein, similar to a bovine brain heparan sulfate-PG isolated previously in our laboratory [26]. The isolated core protein could be visualized with either rabbit anti-glypican or heparan sulfate-PG stub antibody, suggesting that it was a glypican heparan sulfate-PG. Multiple attempts at amino-sequencing of this protein core failed, suggesting it was either blocked at the N-terminus or contained multiple N-termini such as might be expected from a mixture of glypican core proteins. Our attention next turned to the characterization of the heparan sulfate-GAGs in human liver.

The average molecular weight of human liver heparan sulfate-GAGs was comparable with heparan sulfate-GAGs prepared from other animals [19] and somewhat larger than that of heparin. NMR spectroscopy of human liver GAG clearly confirmed it to be an heparan sulfate. Disaccharide analysis showed it to have a lower level of sulfation than heparin but a much higher level of sulfation than bovine kidney heparan sulfate and porcine intestinal heparan sulfate. Interestingly, both similarities and differences were observed when comparing human liver heparan sulfate with heparan sulfate obtained from cultured Hep2G cell (a hepatocytoma cell line). The recoveries of ΔUA-GlcNAc, ΔUA→GlcNS, ΔUA2S→GlcNAc and ΔUA2S→GlcNS6S of human liver heparan sulfate are very different from those of Hep2G cell heparan sulfate (Fig. 4 and Table 1). The content of ΔUA→GlcNAc, ΔUA→GlcNS and ΔUA2S→GlcNAc residues of Hep2G cell heparan sulfate is much higher than that of human liver heparan sulfate. In contrast, the recovery of trisulfated disaccharide unit ΔUA2S→GlcNS6S from human liver heparan sulfate is three times higher than that of Hep2G cell heparan sulfate, and is similar to porcine liver heparan sulfate (Table 1). Since the enzymatic conversion of GlcNAc to GlcNS in heparan sulfate/heparin (associated with disaccharides ΔUA→GlcNAc and ΔUA→GlcNAc6S) is thought to be the first modification of these chains [37], heparan sulfate obtained from cultured Hep2G cells might be "immature" compared to that of human liver. Moreover, unlike the heparan sulfate from Hep2G cells, which showed one population of chains, the heparan sulfate obtained from human liver could be sub-fractionated into two types of heparan sulfate chains of modest and high sulfation.

The results of the current study measure the heparan sulfate present in all liver cell types, e.g., hepatocyte paranchymal cells, Van Kupffer cells, epithelial and fibroblast cells, found in normal human liver including the hepatic cell. The contribution of these various cell types certainly impacts the disaccharide composition and sulfation level when compared to the hepatoma cell line. Furthermore, the hepatoma cell line, while derived from hepatocytes, is a cancer cell line. The decrease in antioxidant enzyme activities in the tumor hepatocytoma cells with a more oxidative stress compared to normal hepatocyte cells [38] may exhaust of thiol donor glutathione, decreasing sulfo-donation by PAPS. Hepatoma cell growth and proliferation are significantly related to the oxidative stress and the extent of reactive oxygen species [39]. The higher level of sulfation in hepatocytoma heparan sulfate disaccharide, compared to bovine kidney heparan sulfate, may be required by this type of cells to facilitate the binding of certain bioactive molecules, like growth factors, that are needed by cells to initiate growth signaling and proliferation. A large family of enzymes including enzymes involved in nucleotide sugar metabolism, polymer formation (glycosyltransferases), and chain processing (sulfotransferases and an epimerase) take part in the biosynthesis of heparan sulfate-PG [40]. The expression of these enzymes can differ greatly between normal hepatic cells and an immortalized hepatoma cell line [41]. The metastasis and increased motility are the basis for malignancy.

Future studies will focus on studying the differences in the interaction of human liver heparan sulfate and heparan sulfate derived from other organs with both growth factors and the ectodomain proteins of microbial pathogens that target the liver [15,22,23].

References

[1] M. Belting, heparan sulfate proteoglycan as a plasma membrane, Trends Biochem. Sci. 28 (2003) 145–151.
[2] P.W. Park, O. Reizes, M. Bernfield, Cell surface heparan sulfate proteoglycans: selective regulators of ligand-receptor encounters, J. Biol. Chem. 275 (2000) 29923–29926.
[3] A.D. Lander, C.S. Stipp, J.K. Ivins, The glypican family of heparan sulfate proteoglycans: major, Perspect. Dev. Neurobiol. 3 (1996) 347–358.
[4] J. Filmus, S.B. Sellick, Glypicans: proteoglycans with a surprise, J. Clin. Invest. 108 (2001) 497–501.
[5] E.M. Selva, N. Perrimon, Role of heparan sulfate proteoglycans in cell signaling and cancer, Adman. Cancer Res. 83 (2001) 67–80.
[6] R.V. Iozzo, J.D. San Antonio, heparan sulfate proteoglycans: heavy hitters in the angiogenesis arena, J. Clin. Invest. 108 (2001) 349–355.
[7] R.V. Iozzo, heparan sulfate proteoglycans: intricate molecules with intriguing functions, J. Clin. Invest. 108 (2001) 165–167.
[8] J. Turnbull, A. Powell, S. Guimond, heparan sulfate: decoding a dynamic multifunctional cell regulator, Trends Cell Biol. 11 (2001) 75–82.
[9] J. Dong, C.A. Peters-Libeu, K.H. Weisgraber, B.W. Segelke, B. Rupp, I. Capila, M.J. Hernaiz, L.A. LeBrun, R.J. Linhardt, Interaction of the N-terminal domain of apolipoprotein E4 with heparin, Biochemistry 40 (2001) 2826–2834.
[10] C. Peters-Libeu, S. Lund-Katz, M. Phillips, S. Wehrli, M.J. Hernaiz, I. Capila, R.J. Linhardt, R. Raffia, Y.M. Newhouse, F. Zhou, K.H. Weisgraber, New insights into the heparan sulfate proteoglycan

binding activity of apolipoprotein E4, J. Biol. Chem. 276 (2001) 39138–39142.
[11] H.G. Bazin, M.A. Marques, A.P. Owens, R.J. Linhardt, K.A. Krutcher, Inhibition of apolipoprotein E-related neurotoxicity by glycosaminoglycans and their oligosaccharides, Biochemistry 41 (2002) 8203–8211.
[12] G.M. Castillo, C. Ngo, J. Cummings, T.N. Wight, A.D. Snow, Perlecan binds to the beta-amyloid proteins (A beta) of Alzheimer's disease, accelerates A beta fibril formation, and maintains A beta fibril stability, J. Neurohemal. 69 (1997) 2452–2465.
[13] Y.L. Lin, H.Y. Lei, Y.S. Lin, T.M. Yeh, S.H. Chen, H.S. Liu, Heparin inhibits dengue-2 virus infection of five human liver cell lines, Antivir. Res. 56 (2002) 93–96.
[14] G. Pradel, S. Garapaty, U. Frevert, Proteoglycans mediate malaria sporozoite targeting to the liver, Mol. Microbiol. 45 (2002) 637–651.
[15] H. Barth, C. Schäfer, M.I. Adam, F. Zhang, R.J. Linhardt, E. Della, F. von Weizsacker, H.E. Blum, T.F. Baumert, Cellular binding of hepatitis C virus envelope glycoprotein E2 requires cell surface heparan sulfate, J. Biol. Chem. 278 (2003) 41003–41012.
[16] J. Mc Clean, The thromboplastic action of cephalin, Am. J. Physiol. 41 (1916) 250–257.
[17] M. Lyon, J.A. Dakin, J.T. Gallagher, Liver heparan sulfate structure, J. Biol. Chem. 269 (1994) 11208–11215.
[18] M.J. Hernáiz, H.O. Yang, N.S. Gunny, R.J. Linhardt, Purification and characterization of heparan sulfate peptidoglycans from bovine liver, Carbohydr. Polym. 48 (2002) 153–160.
[19] T. Toida, H. Yoshida, H. Toyoda, I. Koshiishi, T. Imanari, R.E. Hillman, J.R. Fromm, R.J. Linhardt, Structural differences and the presence of unsubstituted amino groups in heparan sulfates from different tissues and species, Biochem. J. 322 (1997) 499–506.
[20] A.A. Horner, Rat heparins, Biochem. J. 240 (1986) 171–179.
[21] H. Kresse, H. Hausser, R. Schonherr, Small proteoglycans, Experimenta 49 (1993) 403–406.
[22] D. Rathore, T.F. McCutchan, M.J. Hernáiz, L.A. LeBrun, S.C. Lang, R.J. Linhardt, Direct measurement of the interaction of glycosaminoglycans and a heparin hexasaccharide with malaria circumsporozoite protein, Biochemistry 40 (2001) 11518–11524.
[23] Y. Chen, T. Maguire, R.E. Hillman, J.R. Fromm, J.D. Esko, R.J. Linhardt, R.M. Marks, Dengue virus infectivity depends on envelope protein binding to target cell heparan sulfate, Nature Med. 3 (1997) 866–871.
[24] S. Wellnitz, B. Klumpp, H. Barth, S. Ito, E. Depta, J. Dubuisson, H.E. Blum, T.F. Baumert, Binding of hepatitis C virus-like particles derived from infectious clone H77C to defined human cell lines, J. Virol. 76 (2002) 1181–1193.
[25] I. Capila, R.J. Linhardt, Heparin–protein interactions, Angew. Chem., Int. Ed. 41 (2002) 390–412.
[26] Y. Park, G. Yu, N.S. Gunary, R.J. Linhardt, Purification and characterization of heparan sulfate proteoglycans from bovine liver, Biochem. J. 344 (1999) 723–730.
[27] M. Warda, E.M. Gouda, T. Toida, L. Chi, R.J. Linhardt, Isolation and characterization of raw heparin from dromedary intestine: evaluation of a new source of pharmaceutical heparin, Comp. Biochem. Physiol.
[28] C.C. Griffin, R.J. Linhardt, C.L. Van Gorp, T. Toida, R.E. Hillman, R.L. Schubert, S.D. Brown, Isolation and characterization of heparan sulfate from crude porcine intestinal mucosa peptidoglycan heparin, Carbohydr. Res. 276 (1995) 183–197.
[29] H. Toyoda, H. Yamamoto, N. Ogino, T. Toida, T. Imanari, Rapid and sensitive analysis of disaccharide composition in heparin and heparan sulfate by reversed-phase ion-pair chromatography on a 2μm porous silica gel column, J. Chromatogr., A 830 (1999) 197–201.
[30] Y. Liang, M. Haring, P.J. Roughly, R.K. Margolis, R.U. Margolis, Glypican and biglycan in the nuclei of neurons and glioma cells: presence of functional nuclear localization signals and dynamic changes in glypican during the cell cycle, J. Cell Biol. 139 (1997) 851–864.
[31] K. Gu, J. Liu, A. Pervin, R.J. Linhardt, Comparison of the activity of two chondroitin AC lyases on dermatan sulfate, Carbohydr. Res. 244 (1993) 369–377.
[32] R.E. Edens, A. Al-Hakim, J.M. Wailer, D.G. Rethwisch, J. Fareed, R.J. Linhardt, Gradient polyacrylamide gel electrophoresis for determination of molecular weights of heparin preparations and low-molecular-weight heparin derivatives, J. Pharm. Sci. 81 (1992) 823–827.
[33] Z.M. Merchant, Y.S. Kim, K.G. Rice, R.J. Linhardt, Structure of heparin derived tetrasaccharides, Biochem. J. 229 (1985) 369–377.
[34] J.T. Gallagher, A. Walker, Molecular distinctions between heparan sulfate and heparin. Analysis of sulfation patterns indicates that heparan sulfate and heparin are separate families of *N*-sulfated polysaccharides, Biochem. J. 230 (1985) 665–674.
[35] R.J. Linhardt, T. Toida, Role of glycosaminoglycans in cellular communication, Accounts Chem. Res. 37 (2004) 431–438.
[36] D. WuDunn, P.G. Spear, Initial interaction of herpes simplex virus with cells is binding to heparan sulfate, J. Virol. 63 (1989) 52–58.
[37] M. Yanagishita, Cellular catabolism of heparan sulfate proteoglycans, TIGG 10 (1998) 57–63.
[38] Y.J. Sung, C.C. Juan, H.C. Lee, P.H. Yin, C.W. Chi, H.H. Ku, A.F. Li, Y.H. Wei, H.J. Tsay, Oxidative stress is insignificant in N1S1-transplanted hepatoma despite markedly declined activities of the antioxidant enzymes, Nocl, Reports 6 (1999) 1313–1319.
[39] S. Dong-Yun, D. Yu-Ru, L. Shan-Lin, Z. Ya-Dong, W. Lian, Redox stress regulates cell proliferation and apoptosis of human hepatoma through Akt protein phosphorylation, FEBS Lett. 542 (2003) 60–64.
[40] J.D. Esko, S.B. Sellick, Order out of chaos; assembly of ligand binding sites in heparan sulfate, Ann. Rev. Biochem. 71 (2002) 435–471.
[41] T. Nakatsura, Y. Yoshitake, S. Senju, M. Monji, H. Komori, Y. Motomura, S. Hosaka, T. Beppu, T. Ishiko, H. Kamohara, H. Ashihara, T. Katagiri, Y. Furukawa, S. Fujiyawa, M. Ogawa, Y. Nakamura, Y. Nishimura, Glypican-3, overexpressed specifically in human hepatocellular carcinoma, is a novel tumor maker, Biochem. Biophys. Res. Commun. 306 (2003) 16–25.